RSC Advances

PAPER

Cite this: *RSC Adv.*, 2016, **6**, 26757

Species-specific thiol-disulfide equilibrium constants of ovothiol A and penicillamine with glutathione

Arash Mirzahosseini[ab] and Béla Noszál*[ab]

Received 20th January 2016
Accepted 6th March 2016

DOI: 10.1039/c6ra01778a

www.rsc.org/advances

The highly composite acid–base and redox equilibria of thiols can so far be converted into pH-dependent, apparent redox equilibrium constants only. In this work, microscopic redox equilibrium constants were determined to quantify the thiol-disulfide equilibria of biologically important substances in intriguing interactions. The thiol-disulfide redox equilibria of glutathione with ovothiol A and penicillamine were analyzed by quantitative NMR methods to characterize the codependent acid–base and redox equilibria. The directly obtained, pH-dependent, conditional constants were then decomposed to pH-independent, microscopic redox equilibrium constants. These equilibria and the 96 different microscopic redox equilibrium constants are highly influenced by the protonation stage of the adjacent basic moieties. Our data show that equilibrium constants referring to redox systems of covalently identical molecular skeletons, but different acid–base status, can differ by orders of magnitude. In fact, this difference can be as many as 14 orders of magnitude in the glutathione–ovothiol system. This enormous diversity is due primarily to the extreme sensitivity of the ovothiol sulfur to the protonation-evoked electron-withdrawing effects of neighboring basic groups. The thiolate oxidizabilities show close correlation with the respective thiolate basicities and provide sound means for the development of potent agents against oxidative stress.

1. Introduction

Glutathione (γ-L-glutamyl-L-cysteinyl-glycine, GSH) is the single most important non-enzymatic intracellular antioxidant.[1] The reason glutathione works as an ideal redox buffer is its optimal, pH-modulated redox potential, which is not yet thoroughly understood and quantified, and is actually the subject of this and forthcoming papers. Nevertheless, the ubiquitous GSH–GSSG redox system is the most widely studied one.[2,3] It does not require enzyme catalysis to function, and can be applied in aqueous media under a wide range of conditions. These advantages make the GSH–GSSG system a "gold standard" in thiol-disulfide biochemistry; hence, every thiol-containing antioxidant is compared to glutathione.[4] It is a key feature of any thiol-disulfide redox system, however, that only the deprotonated thiol species are active in the redox process, *i.e.* only the anionic thiolate can be oxidized directly[5–8] (Fig. 1A). The redox potential of thiol-containing biomolecules is usually doubly pH-dependent. Primarily, the deprotonated fraction of every thiol depends on the pH of the solution, with strong dependence typically in the 6–11 pH range. Secondarily, the thiolate oxidizability in most biomolecules is modulated by the adjacent basic groups, since protonation of any such group exerts an electron-withdrawing effect on the thiolate. A thiolate has therefore 2^n different, distinct oxidizabilities within a single, covalently unchanged molecular skeleton, if the number of the basic sites in its intramolecular environment is n.[9] Thus, macroscopic physico-chemical parameters cannot characterize the thiolate moiety specifically. A thorough characterization of the thiol-disulfide equilibria can be achieved in terms of species-specific, so-called microscopic parameters, which are, in fact, well-established for acid–base systems.[10,11]

We have recently introduced a method for the determination of pH-independent redox equilibrium constants,[9] and reported their actual values for systems containing glutathione and cysteine, cysteamine, homocysteine, the three best known biological thiols. Here we report the species-specific redox equilibrium constants of glutathione with ovothiol A (OvSH – a highly unusual biomolecule), and penicillamine (PenSH – a thiol-containing drug which was chosen as a comparator molecule, since its molecular skeleton highly resembles that of cysteine, the most commonplace thiol studied); structural formulae in Fig. 1B. Ovothiol A, B, and C are naturally occurring 4-mercaptohistidine derivatives, which differ in the level of methylation at the amino site: latters are mono- and dimethyl derivatives, respectively. Henceforth, our discussion will include ovothiol A only, which will simply be referred to as ovothiol (OvSH). Ovothiol, with four basic moieties and 32 protonation

[a]*Department of Pharmaceutical Chemistry, Semmelweis University, Hőgyes Endre utca 9, H-1092 Budapest, Hungary. E-mail: noszal.bela@pharma.semmelweis-univ.hu; Fax: +36 12170891; Tel: +36 12170891*

[b]*Research Group of Drugs of Abuse and Doping Agents, Hungarian Academy of Sciences, Hungary*

This journal is © The Royal Society of Chemistry 2016

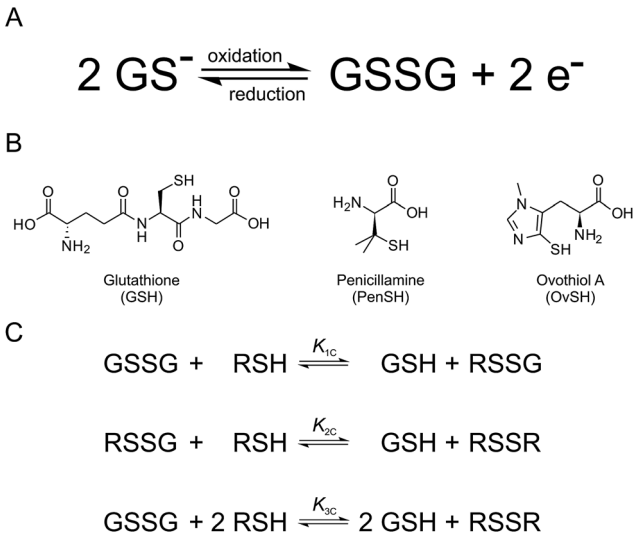

Fig. 1 (A): The thiol-disulfide redox half-reaction between GSH and GSSG. (B): The structural formulae of the studied thiols. (C): The scheme of thiol-disulfide equilibria at the macroscopic level. RSH denotes penicillamine and ovothiol; RSSR denotes their respective homodisulfides; RSSG denotes their respective heterodisulfides formed with glutathione.

microconstants, is one of the richest and most multifaceted chemical entities among all small biomolecules. The extremely rich functionality and the compact electron system in ovothiol feature several peculiarities: ovothiol is doubly zwitterionic at physiological pH; it has strong imidazole–thiolate interactivity; each of its 4 basic sites has 8 significantly different basicities; it has the lowest thiolate protonation constants ever reported.[12] A consequence of the latter property is that the sulfur atom in ovothiol exists nearly throughout the entire pH scale in the anionic form, being thus vulnerable to oxidizing effects. Due to the eight different thiolate protonation constants of ovothiol, the sulfur atom occurs in 8 differently modulated states of electron density; this provides high versatility in antioxidant capability, without any covalent changes in the molecule. The microscopic protonation constants of ovothiol, penicillamine, glutathione and their respective homodisulfides are *sine qua non* components to determine species-specific thiol-disulfide equilibrium constants, and have been reported previously.[12–15]

The general scheme of thiol-disulfide redox equilibria are depicted in Fig. 1C, where RSH and RSSR stand for the reduced and oxidized form of the thiol, and RSSG stands for the heterodisulfide of the corresponding thiol and glutathione. The three conditional equilibrium constants are as follows:

$$K_{1C} = \frac{[GSH][RSSG]}{[RSH][GSSG]} \quad (1)$$

$$K_{2C} = \frac{[GSH][RSSR]}{[RSH][RSSG]} \quad (2)$$

$$K_{3C} = K_{1C}K_{2C} = \frac{[GSH]^2[RSSR]}{[RSH]^2[GSSG]} \quad (3)$$

Since redox and acid–base reactions coexist, K_{1C}, K_{2C}, and K_{3C}, the observed apparent redox equilibrium constants are pH-dependent. In order to get a clear insight into the redox equilibria, purified from the protonation effects, species-specific redox equilibrium constants (k_1, k_2, k_3) had to be introduced. It is clear from eqn (3) that the complete redox transition includes two thiols and two homodisulfides. We therefore confined our efforts to the determination of the K_{3C} macroconstants, and the related k_3 microconstants, the number of which can certainly be numerous. This confinement overcomes the highly complex quantification of the heterodisulfides, which actually improves perspicuity.

2. Experimental section

2.1 Materials

Ovothiol disulfide was synthesized based on a previous work.[16] Glutathione, penicillamine disulfide and all other chemicals were purchased from Sigma-Aldrich (Saint Louis, MO, USA) and used without further purification.

2.2 Preparation of solutions

Acidic (pH = 0.85) and basic (pH = 13.15) stock solutions (GSH + ovothiol disulfide or penicillamine disulfide) were prepared in an 815-PGB glove box (Plas-Labs Ic., Lansing, MI, USA) under N_2 atmosphere to preclude oxidation by air. The concentrations of the reagents were optimized for quantitative NMR at around 15 mmol L^{-1}. Sixteen ovothiol–glutathione solutions with different pH and sixteen penicillamine–glutathione solutions with different pH (for pH values see Table 1) were prepared by mixing the acidic with the basic stock solutions. D_2O, DSS (sodium 4,4-dimethyl-4-silapentane-1-sulfonate), and a pH indicator, which also served as a concentration standard, were added to the solutions. The concentration of the pH indicators/concentration standards were comparable to the analyte concentrations in the final samples, and included: dichloroacetic acid for pH 0–2, formic acid for pH 2–4, imidazole for pH 5–9, *tert*-butylamine for pH 9–12. The samples were protected from sunlight and kept in the glove box under N_2 atmosphere for 7 days, until the reactions in all the samples had reached equilibrium. The samples were transferred into the NMR tubes under N_2 atmosphere for the measurements and the NMR tubes were sealed with a plastic tube cap and silicone film under positive gas pressure.

2.3 NMR spectroscopy measurements

NMR spectra were recorded on a Varian 600 MHz spectrometer at 25.0 ± 0.1 °C. The solvent in every case was an aqueous solution with $H_2O : D_2O$, 95 : 5, v/v (0.15 mol L^{-1} ionic strength), using DSS as the reference compound. The sample volume was 600 μL, pH values were determined by internal indicator molecules optimized for NMR.[17,18] ^1H NMR spectra were recorded with the WET solvent suppression sequence (number of transients = 64, number of points = 16 384, acquisition time = 851.968 ms, relaxation delay = 15 s).

This journal is © The Royal Society of Chemistry 2016

Table 1 Conditional redox equilibrium constants. The conditional redox equilibrium constants of penicillamine– and ovothiol–glutathione thiol-disulfide systems. The uncertainties in the pH and log K_{3C} values are 0.01–0.02 and 0.002–0.004, respectively

Penicillamine		Ovothiol	
pH	log K_{3C}	pH	log K_{3C}
0.84	−0.155	0.85	−0.850
1.26	−0.119	1.24	−1.402
1.52	−0.056	1.78	−2.444
1.85	−0.027	2.43	−2.924
2.31	−0.009	3.02	−3.889
2.91	−0.086	4.11	−5.278
3.25	−0.137	5.09	−5.793
3.41	−0.237	5.61	−6.124
5.54	−0.310	6.28	−5.875
6.40	−0.328	7.21	−6.267
7.67	−0.456	8.08	−5.851
8.88	−1.046	9.20	−5.412
9.67	−0.745	9.42	−5.050
9.90	−0.699	10.28	−4.611
10.44	−1.398	11.34	−3.972
11.88	0.161	11.95	−3.878

2.4 Data analysis

For the analysis of quantitative NMR measurements, the peak fitting algorithm (without apodization) of the ACD/NMR Processor Academic Edition v12.01 software package (Advanced Chemistry Development, Toronto, ON, Canada) was used. For the regression analyses, the software Origin Pro 8 (OriginLab Corp., Northampton, MA, USA) was used. The standard deviations of the peak areas obtained by fitting Lorentzian peak shapes, the error of pH determination, and the standard errors of the microscopic protonation constants[12–15] were used to calculate the Gaussian propagation of uncertainty to the redox equilibrium constants derived in the Results chapter. In practice, the measured ^{1}H NMR spectra were fitted to Lorentzian curves in the frequency domain using the curve fitting algorithm of ACD 1D NMR Processor. The Fourier number was always set to maximum, automatic baseline and phase correction, and no apodization was used. Using the chemical shift-pH profiles determined previously[12–15] the chemical shifts of the various nuclei in the coexisting molecules (*e.g.* OvSH, GSH, OvSSOv, GSSG) at a given pH could be predicted (sample spectra are depicted in Fig. 2). For the sake of simplicity, whenever possible the following characteristic peaks were observed: α-glutamyl-, α-cysteinyl-, glycinyl proton of GSH and GSSG; imidazolyl H_2-, α-proton of OvSH, OvSSOv; CH_3-, α-proton of PenSH, PenSSPen. In order to calculate the concentration of the species, the integrals of the fitted peaks were related to the integral of the pH indicator peak, which also served as concentration standard. The indicators were chosen so that their peaks were always discernable. When no any peak was discernable for one of the species due to overlapping signals, its concentration was calculated using the concentration of the stock solutions and the law of conservation of mass.

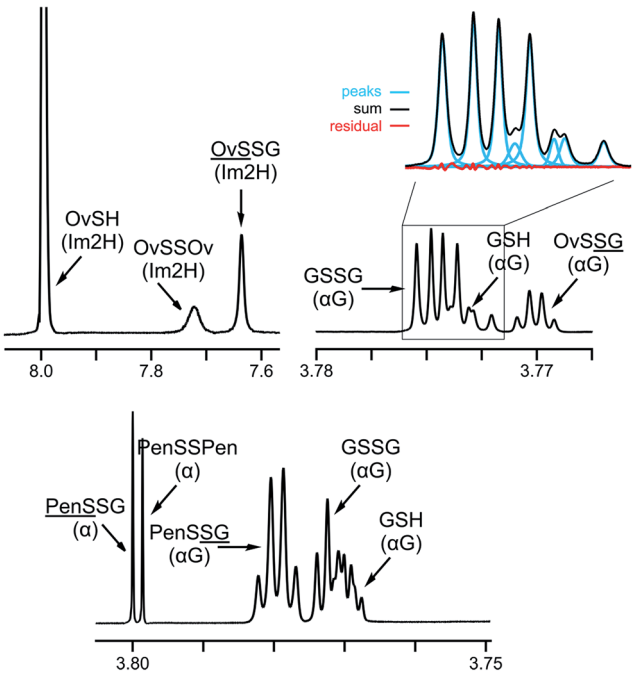

Fig. 2 The expanded ^{1}H NMR spectra of samples containing ovothiol–glutathione mixtures (top, with example of peak fitting result, pH = 9.20) and penicillamine–glutathione mixtures (bottom, pH = 8.88).

3. Results

3.1 Description of protonation microequilibria

The description and elucidation of protonation microequilibria for multibasic compounds is extensively elaborated on in the review article of Szakács *et al.*;[11] only a brief summary on relevant thiol and disulfide protonation microequilibria is given below. Fig. 3 represents the species-specific protonation scheme of a triprotic thiol and its homodisulfide (such is PenSH/PenSSPen) and Fig. 4 represents the species-specific protonation scheme of a tetraprotic thiol and its homodisulfide (such is GSH/GSSG and OvSH/OvSSOv). Macroequilibria (top lines) indicate the stoichiometry of the successively protonated ligand and the stepwise macroscopic protonation constants. In the microspeciation schemes, the different microspecies with their one-letter symbols (a, b, c …), and the microscopic protonation constants are depicted (k^N, k^S_N …). The superscript at k for any microconstant indicates the protonating group while the subscript (if any) shows the site(s) already protonated. S, N, O, G and E symbolize the thiolate, amino, carboxylate (in PenSH and PenSSPen), glycinyl carboxylate, and glutamyl carboxylate (in GSH and GSSG after their one-letter symbol) sites, respectively. In Fig. 4, for the case of ovothiol the symbols G and E should be replaced with Im (imidazole) and O (carboxylate). The acid–base macro- and microequilibria are inevitable constituents in the evaluation of the species-specific, pH-independent redox equilibrium constants, as shown in eqn (9) and (10). Some protonation constant examples for penicillamine are shown below:

$$K_2 = \frac{[H_2L]}{[HL^-][H^+]} \quad (4)$$

$$\beta_3 = K_1K_2K_3 = \frac{[H_3L^+]}{[L^{2-}][H^+]^3} \quad (5)$$

$$k^N = \frac{[b]}{[a][H^+]} \quad (6)$$

where K_1, K_2, K_3, are successive macroconstants, β_3 is one of the cumulative macroconstants, k^N is the microconstant representing the amino protonation in penicillamine, when its carboxylate and thiolate sites are unprotonated. The concentrations of the various macrospecies comprise the sum of the concentration of those microspecies that contain the same number of protons, for example in GSH:

$$[H_2L^-] = [F] + [G] + [H] + [I] + [J] + [K] \quad (7)$$

3.2 Description of redox microequilibria

For the thiol-disulfide redox equilibria, only the apparent (or conditional) equilibrium constants (K_{3C}) can be directly determined, by measuring the equilibrium concentration of RSH, GSH, RSSR, and GSSG in the reaction mixtures. These apparent equilibrium constants are valid at the particular pH of the measurement only, since the protonation status and the concomitant equilibrium concentration of each of the RSH, GSH, RSSR, and GSSG macrospecies change differently with pH. The equilibrium concentration of the four macrospecies above can be measured as the integral of a characteristic, discernable NMR peak of the species in question. The concentration of the macrospecies can be written as the sum of the microspecies of the same number of bound protons, as shown in eqn (7) for

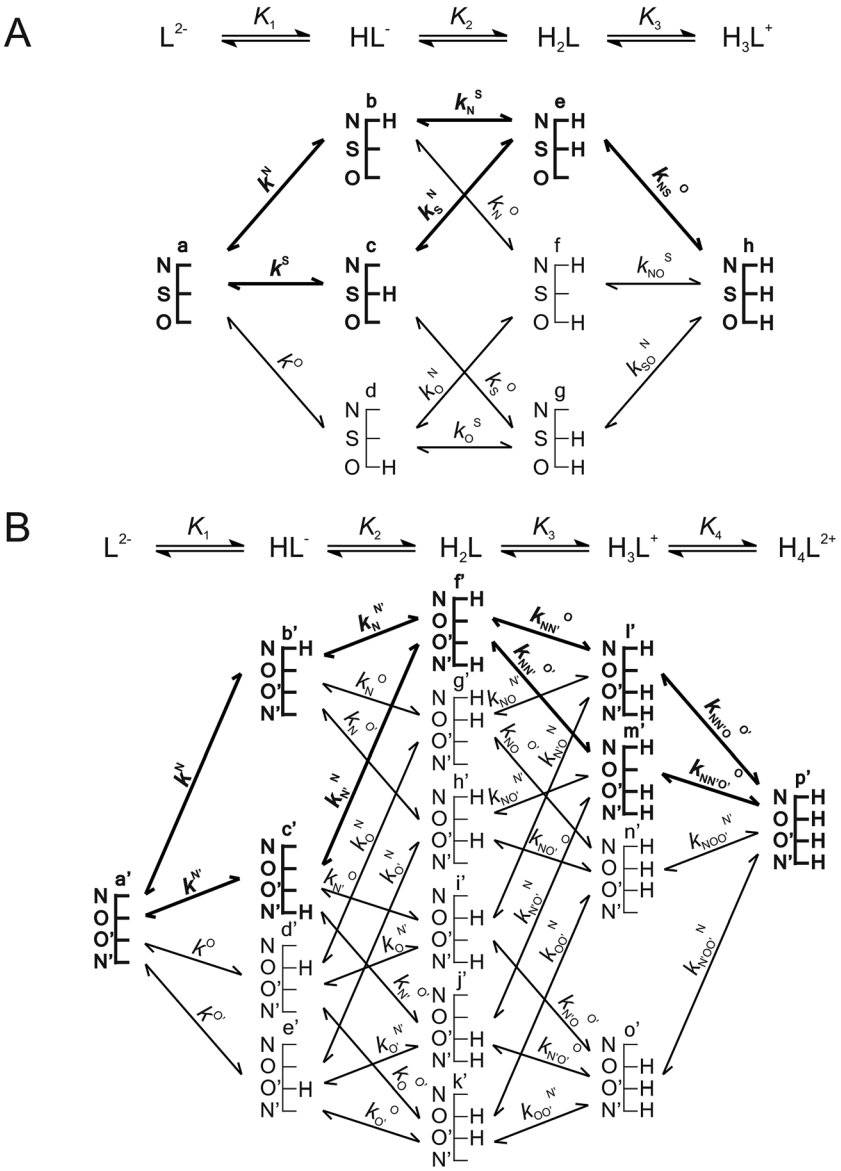

Fig. 3 The protonation macro- and microequilibrium schemes of PenSH (A) and PenSSPen (B) in terms of stepwise macroscopic protonation constants (K_1, K_2, K_3 …), where L^{2-}, HL^-, *etc.* are the successively protonating ligands (top lines). Below are the species-specific protonation schemes in terms of microspecies (a, b, c …) and microscopic protonation constants (k^N, k^S_N …). The components of the major pathways are in bold.

This journal is © The Royal Society of Chemistry 2016

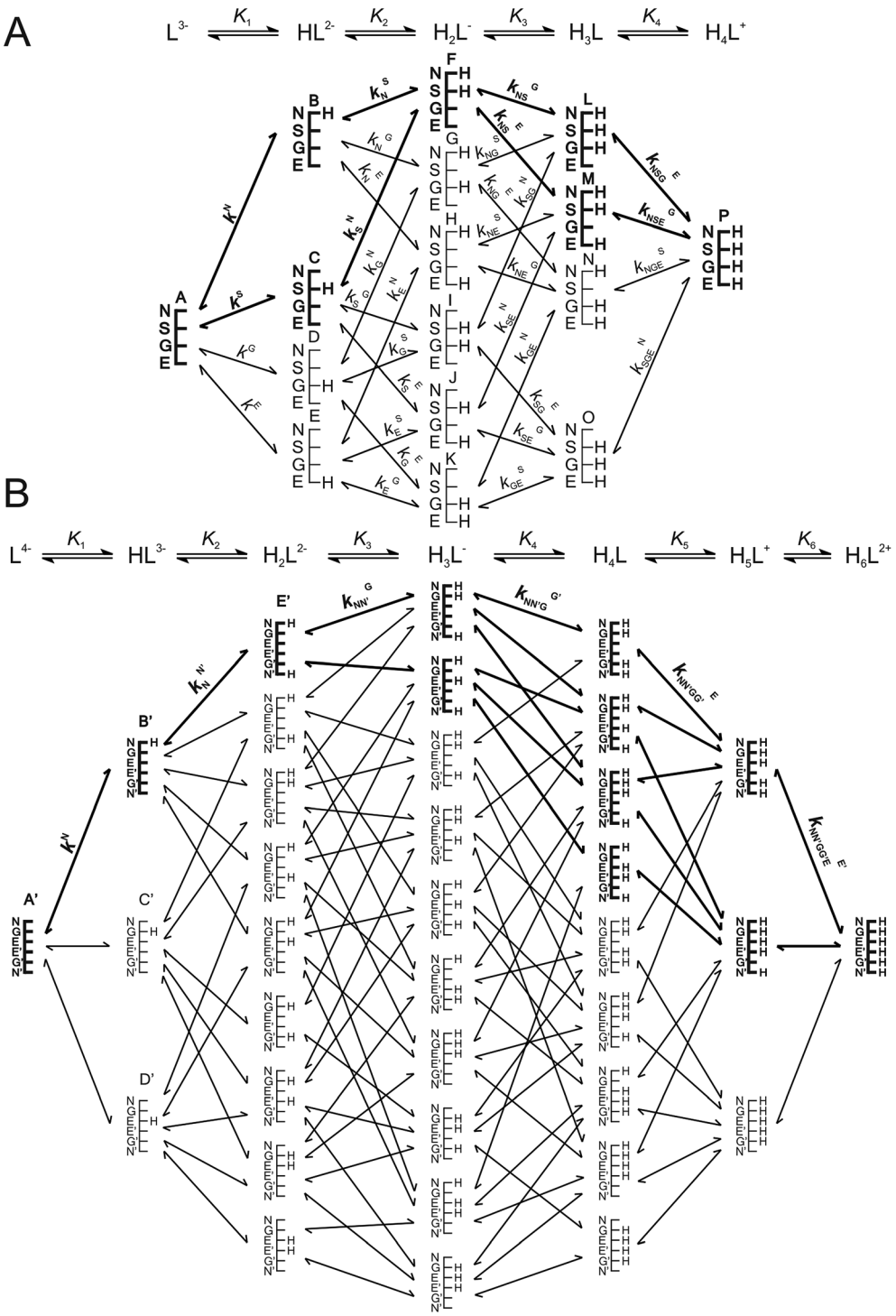

Fig. 4 The protonation macro- and microequilibrium schemes of GSH (A) and GSSG (B) in terms of stepwise macroscopic protonation constants (K_1, K_2, K_3 …), where L^{3-}, HL^{2-}, *etc.* are the successively protonating ligands (top lines). Below are the species-specific protonation schemes in terms of microspecies (A, B, C …) and microscopic protonation constants (k^N, k^S_N …). For GSSG, only non-identical microspecies and microconstants are shown, and only a few of the microconstants are depicted. The components of the major pathways are in bold. The protonation schemes of OvSH and OvSSOv are identical to the depicted schemes except Im (imidazole) and O (carboxylate) moieties are present instead of G (glycincyl carboxylate) and E (glutamyl carboxylate).

H_2L^- of GSH. The pH-dependent, apparent constants can be decomposed into pH-independent, species-specific equilibrium constants, the number of which is large, but definite. For example, the thiolate moiety in penicillamine is adjacent to two other basic sites; the amino and the carboxylate groups. Therefore, the thiolate-bearing penicillamine microspecies exist in 4 different protonation states. Concurrently, the thiolate groups in the 4 different microspecies will be in 4 different

electrostatic environments, thus having 4 different oxidizabilities. Considering the opposite direction of the redox equilibrium, GSH with an amino and two carboxylate sites occur in 8 different thiolate-bearing microspecies with 8 different electron densities on its sulfur. This leads to $4 \times 8 = 32$ different microscopic redox equilibria between penicillamine and glutathione. To epitomize the determination of microscopic redox equilibrium constants (k_3) from the conditional equilibrium constants (K_{3C}), the calculation of the k_3^{bB} for the reaction involving the b microspecies of penicillamine, the corresponding f′ penicillamine disulfide microspecies, the B glutathione microspecies, and the corresponding E′ glutathione disulfide microspecies will be demonstrated. Note that b and B thiolate microspecies determine the disulfide microspecies as f′ and E′, since these are the microspecies with identical side-chain protonation status. Superscripts b and B (in k_3^{bB}) therefore unambiguously identify all the 4 microspecies in the micro-equilibrium in question.

This example of the pH-independent, microscopic thiol-disulfide equilibrium constants is expressed by eqn (8):

$$k_3^{bB} = \frac{[B]^2[f']}{[b]^2[E']} \quad (8)$$

As shown in eqn (9), the [b], [E′], [B], and [f′] species-specific concentrations can be obtained as the product of total species concentration and the relative abundance of the respective microspecies. The relative abundance of the microspecies in turn, is a function of pH and the microscopic protonation constants. For the b penicillamine microspecies, the concentration can be written as follows:

$$[b] = [PenSH]\chi_b = [PenSH]\frac{k^N[H^+]}{1 + \beta_1[H^+] + \beta_2[H^+]^2 + \beta_3[H^+]^3} \quad (9)$$

where [PenSH] is the total solution concentration of penicillamine, χ_b is the relative abundance of microspecies b (*i.e.* χ_b = [b]/[PenSH]), k^N is the microscopic protonation constant of penicillamine involved in the formation of microspecies b, and β is the cumulative protonation constant of penicillamine. Introducing analogous equations as eqn (9) for the concentrations of every microspecies in k_3^{bB}, the equation of the microscopic equilibrium constant can be written as follows:

$$k_3^{bB} = \frac{[B]^2[f']}{[b]^2[E']} = \frac{[GSH]^2\chi_B^2[PenSSPen]\chi_{f'}}{[PensH]^2\chi_b^2[GSSG]\chi_{E'}} = K_{3C}\frac{\chi_B^2\chi_{f'}}{\chi_b^2\chi_{E'}} \quad (10)$$

Thus, if K_{3C}, the apparent equilibrium constant and the 4χ values (as functions of the protonation constants and pH) have previously been determined, the k_3^{bB} value and all the analogous, pH-independent, species-specific redox microconstants can be calculated. The protonation scheme of a polybasic, non-symmetrical molecule certainly contains more favorable (bold pathways in Fig. 3 and 4) and less favorable pathways. The extremely minor protonation microspecies contribute to a negligible fraction of the analyte signal. Nevertheless, the major microspecies are not necessarily the reactive microspecies in the

Table 2 Species-specific redox equilibrium constants of glutathione with penicillamine and ovothiol in log units. Each column corresponds to a penicillamine or ovothiol microspecies, the one-letter symbols of which are described in Fig. 2 (the sites of protonation are depicted in Fig. 5). On the other hand, each row corresponds to a glutathione microspecies. Note, that a certain pair of RSH and GSH microspecies unambiguously determines the RSSR and GSSG microspecies that also take part in the thiol-disulfide equilibrium. For example, log k_3^A of the penicillamine–glutathione system has the value of 0.19, and can be found in the left uppermost corner of the penicillamine box. The uncertainties in the log k_3 values are 0.01–0.03

Site(s) of protonation and one-letter symbols of thiolate microspecies																
		Penicillamine					Ovothiol									
		—	Amino	Carboxylate	Amino carboxylate		—	Imidazole	Amino	Carboxylate	Imidazole amino	Imidazole carboxylate		Amino carboxylate		Imidazole amino carboxylate
Glutathione		a	b	d	f		A	B	C	D	F	G		I		L
—	A	0.19	−2.24	−1.40	−4.51		−5.26	−12.52	−7.65	−6.55	−17.26	−12.80		−9.82		−17.85
Amino	B	0.51	−1.90	−1.07	−4.21		−4.94	−12.13	−7.33	−6.22	−16.04	−12.42		−9.70		−16.71
Gly carboxylate	D	0.57	−1.81	−1.06	−4.16		−4.88	−12.10	−7.25	−6.12	−17.12	−12.35		−9.54		−17.22
Glu carboxylate	E	0.43	−1.96	−1.16	−4.38		−5.02	−12.27	−7.44	−6.41	−17.02	−12.57		−9.88		−17.42
Amino gly carboxylate	G	1.25	−1.15	−0.35	−3.49		−4.21	−11.45	−6.63	−5.48	−16.02	−11.76		−8.96		−16.24
Amino glu carboxylate	H	0.95	−1.46	−0.67	−3.75		−4.50	−11.74	−6.96	−5.75	−16.35	−12.01		−9.06		−16.49
Both carboxylates	K	1.05	−1.39	−0.55	−3.69		−4.40	−11.62	−6.83	−5.65	−16.09	−11.92		−8.96		−16.35
Amino both carboxylates	N	1.93	−0.43	0.32	−2.80		−3.52	−10.78	−5.92	−4.67	−15.34	−11.06		−8.28		−15.34

This journal is © The Royal Society of Chemistry 2016

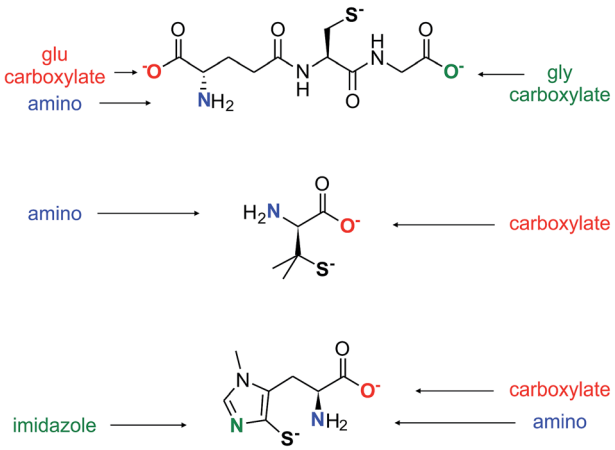

Fig. 5 The protonation sites of the thiolate forms of glutathione, penicillamine, and ovothiol.

highly specific, structure-controlled biochemical reactions. Also, the theoretical discussion of microequilibria can only be exact by considering the complete scheme of protonation. For thiol-disulfide systems there is also a practical aspect: if only the major thiolate protonation pathways are considered, thiol-disulfide equilibria (which take place *via* the *thiolate* form) could not be defined accurately for acidic media where the thiol form overwhelmingly dominates over the thiolate form.

3.3 Determination of thiol-disulfide equilibrium constants

The conditional equilibrium constants were calculated from the concentrations in the equilibrium reaction mixtures according to eqn (3). The conditional redox equilibrium constant values are listed in Table 1.

The microscopic redox equilibrium constants were calculated from the conditional equilibrium constants using analogous equations as eqn (10). Obviously, the conditional equilibrium constants were measured at different pH media, all of which theoretically afford the same value for a certain microscopic equilibrium constant. However, each microscopic redox equilibrium constant was calculated at pH values where the corresponding eqn (10) is well-conditioned, *i.e.* the mole fractions of the involved microspecies are near-maximal. For k_3^{bB} the optimal pH of determination are 5.54, 6.40, 7.67, 8.88 (see Table 1). The mean of the calculated microscopic redox equilibrium constants are listed in Table 2. The correlation between the $\log k_3^{XY}$ and $\Delta\log k$ (the difference in species-specific protonation constants of the involved RSH and GSH thiolates) are depicted in Fig. 5.

4. Discussion

The highly interwoven acid–base and redox properties of the GSH/GSSG–RSH/RSSR system can be decomposed into elementary, component equilibria if (a) the species-specific protonation constants of GSH, GSSG, RSH, and RSSR are determined, and (b) the conditional equilibrium constants of the pH-dependent redox equilibria are also quantified. In this work the thiol-disulfide equilibria of glutathione with ovothiol and penicillamine were characterized in terms of conditional and species-specific equilibrium constants. As anticipated, the dissection of conditional equilibria into elementary redox ones in biological thiol-disulfide systems reveals significant differences between reactions of apparently highly similar, covalently identical reactants, improving thus our understanding of redox homeostasis and providing new means to influence it. As Table 2 reveals, this is all the more important in light of the highly complex, parallel protonation equilibria of these multibasic biomolecules: not only the protonation of the thiolate, its protonation fraction, and the concomitant redox behavior will be very sensitive to minor pH changes, but the protonation state of neighboring basic moieties can influence the redox behavior by various inductive effects on the thiolate moiety. The correlation between thiolate basicity and redox behavior in this paper is in excellent agreement with the previously published claims that thiolate basicity and oxidizability are proportional parameters.[3]

Major trends among the k_3^{XY} redox microconstants in Table 2 are that their values markedly decrease as the strength and number of electron-withdrawing moieties increases on the ovothiol/penicillamine species, and *vice versa* on the glutathione species. Gradually protonating side-chain sites and the concomitantly decreasing electron density at the thiolate site bring about this change in redox microconstants. Such effects in the side-chain protonation are strongest in ovothiol (*e.g.* $k_3^{DN} \gg k_3^{FA}$), due to the proximity and strong interaction of the imidazole moiety with the thiolate. Protonation of the ovothiol imidazole site decreases the k_3^{XY} value by a factor of 10^7, while protonation of the amino and carboxylate exert an effect of the same direction by a factor of 250 and 20, respectively. Effects of the glutathione side-chain protonation can be observed in columns downward as increasing $\log k_3^{XY}$ values. Even though in glutathione three groups protonate in the vicinity of its thiolate, their cumulative effect is typically less than 200 fold on the equilibrium constants. Upon comparing k_3^{AN} and k_3^{LA} ($10^{-3.52}$ and $10^{-17.85}$) in the ovothiol–glutathione system, the difference between these values is some 14 orders of magnitude, indicating that side-chain protonations can immensely modify thiol-disulfide equilibria, while covalent structures remain exactly the same. The trends in k_3^{XY} redox microconstants of penicillamine show good agreement with the values of cysteine.[9] The similar molecular skeleton of penicillamine and cysteine differ only in the presence of two methyl groups in penicillamine; surely the consistently lower thiolate microscopic protonation constants of penicillamine result in lower redox microconstants. The trends among the 32 k_3^{XY} redox microconstants of penicillamine are that the values generally increase downwards and leftwards. In fact in the penicillamine box of Table 2, the largest value appears in the left bottom corner, while the smallest value can be found in the right uppermost corner. Protonation of the amino site decreases k_3^{XY} by a factor of 250 in penicillamine, while the same effect is 500 in cysteine. Protonation of the carboxylate has an effect of 40 and 80 in penicillamine and cysteine, respectively. Such effects in the side-chain protonation are stronger for the amino site since it is located closer to the thiolate moiety compared to the carboxylate. Furthermore, the lower thiolate basicities in penicillamine and the lower side-chain

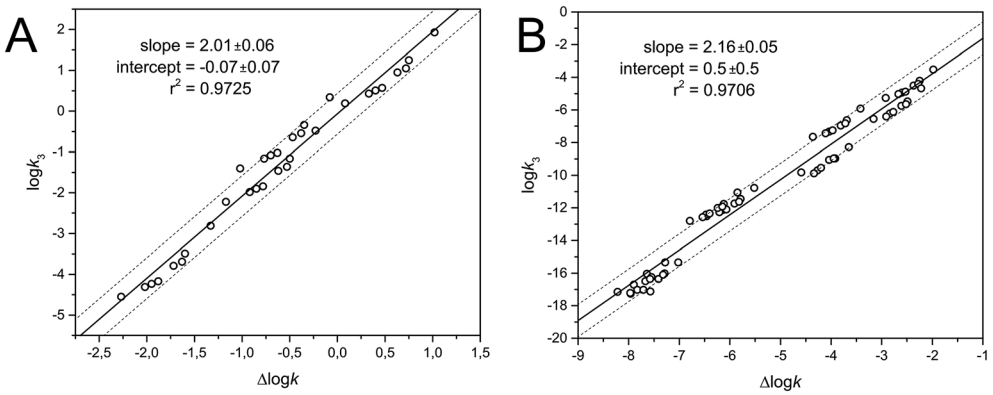

Fig. 6 The correlation between species-specific redox equilibrium constants (log k_3^{xY}) and the difference of species-specific thiolate protonation constants for the involved RSH and GSH microspecies (Δlog *k*); (A) for penicillamine and (B) for ovothiol. The Δlog *k* values were calculated from the species-specific protonation constants previously determined.[12–15]

protonation effect on the redox constants can be best explained with the shielding effect of the two bulky methyl groups cramped around the thiolate.

The strong correlation between the species-specific thiolate protonation constants and species-specific redox equilibrium constants (Fig. 6A and B) confirm the assumption that the thiol-disulfide redox reactions proceed *via* the thiolate form. As the electron density around the thiolate moiety increases, the proton binding affinity and oxidizability (inversely proportional to electron affinity) of the thiolate should increase proportionally, since both processes are governed by electron-density effects. The linear relationship between log *k* thiolate protonation microconstants and log k_3^{xY} redox equilibrium constants indicates that the acid–base and redox equilibria have been broken down to elementary reactions. The slope of the correlation is consistent with those of cysteamine, cysteine, and homocysteine (mean value: 2.11 ± 0.03),[9] this also supports the hypothesis that these acid–base and redox processes are driven by the same force. In the future we intend to determine the species-specific standard redox potentials (E°) of the various GSH microspecies, which can also be done indirectly only. The calculation of the species-specific redox potentials for the redox half-reaction of each thiol microspecies will enable the independent evaluation of these processes from the redox equilibrium partner.

5. Conclusion

The pH-dependent and 96 pH-independent equilibrium constants of the thiol-disulfide redox reactions between glutathione and two important biological thiols were determined. The pH-independent species-specific redox equilibrium constant implemented characterize the redox processes at the microspecies level. The species-specific equilibrium constant values provide sound means to predict thiolate oxidizabilities, a key parameter to understand and influence oxidative stress.

Acknowledgements

This research was supported by TÁMOP 4.2.1.B-09/1/KMR and OTKA T 73804. The authors report no conflict of interest.

References

1 N. S. Kosower and E. M. Kosower, *Int. Rev. Cytol.*, 1978, **54**, 109–160.
2 W. J. Lees and G. M. Whitesides, *J. Org. Chem.*, 1993, **58**, 642–647.
3 K. K. Millis, K. H. Weaver and D. L. Rabenstein, *J. Org. Chem.*, 1993, **58**, 4144–4146.
4 D. A. Keire, E. Strauss, W. Guo, B. Noszál and D. L. Rabenstein, *J. Org. Chem.*, 1992, **57**, 123–127.
5 R. P. Szajewski and G. M. Whitesides, *J. Am. Chem. Soc.*, 1980, **102**, 2011–2026.
6 I. M. Kolthoff, W. Stricks and R. C. Kapoor, *J. Am. Chem. Soc.*, 1955, **77**, 4733–4739.
7 L. Eldjarn and A. Pihl, *J. Am. Chem. Soc.*, 1957, **79**, 4589–4593.
8 J. M. Wilson, R. J. Bayer and D. J. Hupe, *J. Am. Chem. Soc.*, 1977, **99**, 7922–7926.
9 A. Mirzahosseini, M. Somlyay and B. Noszál, *J. Phys. Chem. B*, 2015, **119**, 10191–10197.
10 N. Bjerrum, *Z. Phys. Chem. Stoechiom. Verwandschaftsl.*, 1923, **106**, 219–241.
11 Z. Szakács, M. Kraszni and B. Noszál, *Anal. Bioanal. Chem.*, 2004, **378**, 1428–1448.
12 A. Mirzahosseini, G. Orgován, S. Hosztafi and B. Noszál, *Anal. Bioanal. Chem.*, 2014, **406**, 2377–2387.
13 A. Mirzahosseini, G. Orgován, G. Tóth, S. Hosztafi and B. Noszál, *J. Pharm. Biomed. Anal.*, 2015, **107**, 209–216.
14 A. Mirzahosseini, A. Szilvay and B. Noszál, *Chem. Phys. Lett.*, 2014, **610–611**, 62–69.
15 A. Mirzahosseini, M. Somlyay and B. Noszál, *Chem. Phys. Lett.*, 2015, **622**, 50–56.
16 A. Mirzahosseini, S. Hosztafi, G. Tóth and B. Noszál, *ARKIVOC*, 2014, **6**, 1–9.
17 Z. Szakács, G. Hägele and R. Tyka, *Anal. Chim. Acta*, 2004, **522**, 247–258.
18 G. Orgován and B. Noszál, *J. Pharm. Biomed. Anal.*, 2011, **54**, 958–964.

 This journal is © The Royal Society of Chemistry 2016